



HAL
open science

Ageing of different biodegradable polyesters blends mechanical and hygrothermal behavior

Vincent Berthe, Laurent Ferry, Jean-Charles Benezet, Anne Bergeret

► To cite this version:

Vincent Berthe, Laurent Ferry, Jean-Charles Benezet, Anne Bergeret. Ageing of different biodegradable polyesters blends mechanical and hygrothermal behavior. *Polymer Degradation and Stability*, 2010, 95 (3), pp.262-269. 10.1016/j.polymdegradstab.2009.11.008 . hal-03236170

HAL Id: hal-03236170

<https://imt-mines-ales.hal.science/hal-03236170>

Submitted on 25 May 2022

HAL is a multi-disciplinary open access archive for the deposit and dissemination of scientific research documents, whether they are published or not. The documents may come from teaching and research institutions in France or abroad, or from public or private research centers.

L'archive ouverte pluridisciplinaire **HAL**, est destinée au dépôt et à la diffusion de documents scientifiques de niveau recherche, publiés ou non, émanant des établissements d'enseignement et de recherche français ou étrangers, des laboratoires publics ou privés.

Ageing of different biodegradable polyesters blends mechanical and hygrothermal behavior

V. Berthé, L. Ferry, J.C. Bénézet, A. Bergeret*

Centre des Matériaux de Grande Diffusion, Ecole des Mines d'Alès, 6 avenue de Clavières, 30319 ALES Cedex, France

A B S T R A C T

The aim of this study is to better understand the performance of binary blends of biodegradable polyesters when exposed to hygrothermal ageing, in order to overcome some of their limitations such as water resistance. For this, blends have been prepared by extrusion using two P(L)LA (L-poly-(lactic acid)) of different molecular weights and P ϵ CL (poly- ϵ -caprolactone). Mechanical properties over ageing are reported and compared to pure P(L)LA. Blending P ϵ CL to P(L)LA allowed to improve P(L)LA initial resilience. During ageing, crystallinity increase seemed to lower water uptake at short ageing times, while osmotic cracking was found to possibly occur in pure P(L)LA for long ageing times, thus increasing water uptake. Besides, P(L)LA/P ϵ CL blends water uptake remained constant over ageing. Finally, while P(L)LA resilience decrease could be related to chain scission, blend aptitude to elongation decrease was related to interphase decohesion, at long ageing times. Results showed P(L)LA molecular weight influence on both initial mechanical properties and water uptake.

Keywords:

Poly lactide
Poly- ϵ -caprolactone
Melt blending
Swelling behavior
Hygrothermal ageing

1. Introduction

Ecological issues such as garbage and waste management have to be faced up to. The need to develop biologically degradable plastics and products that may be composted is now tremendous. Aliphatic polyesters are an important family of biodegradable materials. In particular P ϵ CL [1,2] and P(L)LA [3,4] have been widely studied for their usefulness in biomedical applications. Indeed, aliphatic polyesters have a large field of application, with medical care, agricultural and packaging being the most widely researched fields. This is why there is intense scientific interest in multiphase aliphatic polyester blends [5,6] or alloys, since there are potential opportunities for combining their attractive features into a single one. Many publications attempted to enlarge P(L)LA applicability such as improving both elongation and resilience [7,8].

P(L)LA being brittle, its elongation at break can be improved by plasticizing [9] while improvement of impact strength was reported by blending [5,6,10]. Concerning plasticization, P(L)LA being semicrystalline, the plasticizers are incorporated primarily into the amorphous parts [9]. But, as a common defect of the P(L)LA plasticizers, the migration of plasticizer molecules to the material surface is a practical obstacle to their application [11]. Yet, concerning blending and impact modification, most commercial

polymers that have been blended to P(L)LA do not to diffuse at the material surface during ageing. Still, most of those polymers are not biodegradable: low-density-poly-ethylene [12], polyisoprene [13], poly-ethylene-co-acrylic [14].

P(L)LA has also been blended to many polymers among which aliphatic polyesters which are biodegradable P(D)LA (D-poly-(lactic acid)) [15], P ϵ CL [16], PBAT (poly-butylene-adipate-co-terephthalate) [17], PHBV (poly-3-hydroxydutyrate-co-3-hydroxyvalerate) [18], PHBV/PHH (poly-3-hydroxydutyrate-co-3-hydroxyvalerate-co-3-hydroxyhexanoate) [19], PBS (poly-butylene-succinate) [20], PES (poly-ethylene-succinate) [21] and some of their copolymers [22]. One should have in mind that those blend mechanical properties may also be dependent on both the molding process and the molecular weight of the materials [23]. In addition, control of water sensitivity and biodegradability of P(L)LA was studied when blended to P ϵ CL [24]. Poly lactide blends with P ϵ CL phase-separate [16,22,25–32]. P(L,D)LA (L,D-poly-(lactic acid))/P ϵ CL blends [16,29,31] show a lower critical solution temperature. The morphology, structure, and physical properties of P(L)LA/P ϵ CL blends were observed for blends prepared by solution-casting [6,22]. Concerning the P(L)LA/P ϵ CL blends prepared by melt mixing, the thermal properties and phase morphology of P(L)LA/P ϵ CL were found to reflect an immiscible behavior, even though it was suggested, using Dynamical Mechanical Analysis, that P ϵ CL may be partially miscible in P(L)LA-rich phase (but only up to 1 wt% P ϵ CL) [35]. Basing our choice on literature dealing with P(L)LA impact resistance improvement [28,29,33], we studied one specific P(L)LA based blend: P(L)LA/P ϵ CL w:w 80/20.

* Corresponding author. Tel.: +33 4 66 78 53 44; fax: +33 4 66 78 53 65.
E-mail address: Anne.Bergeret@ema.fr (A. Bergeret).

Some applications of P(L)LA require a deep knowledge about the durability and predictability of the macroscopic properties. In this context, we performed hygrothermal ageing. Samples exposed to humidity and temperature accurately simulate most P(L)LA application shelf-life environment [34]. The rate of P(L)LA hydrolysis increases markedly above T_g [34] and also as the hydrolysis proceeds, presumably due to the production of hydrophilic groups (alcohol, acid...) [35]. Likewise, hydrophilic molecules and functional groups such as lactide and carboxylic acid, whose concentration is proportional to degradation, increase the level of moisture. Morphology may affect water permeation through crystallinity but also by the presence of microvoids or porosity [36]. In the case of microvoids, water migrates into the material and thereby enhances the rate of hydrolysis. Still water diffusion rate is much higher than that of hydrolysis, thus the impact of microvoids is small since this phenomenon is hydrolysis-controlled. Anyway, localized regions of high water absorption may cause mechanical stresses due to increased osmotic pressure. In the case of compatibilized P(L)LA/PεCL blend, water resistance is known to be greater than that of neat P(L)LA [24]. Concerning P(L)LA and P(L)LA based blends mechanical properties, literature highlighted that water absorption induces severe degradations [27]. The main parameters of those properties are physical modifications, i.e. plasticization [26], and chemical modifications, i.e. hydrolysis [26], but also debondings affecting blend interfaces [26]. In addition, water absorption is highly dependent on crystallinity [27]. Talking about hydrolysis of P(L)LA, this reaction is influenced by temperature [28], pH [37], chemical structure [38] (cross-linking, co-monomers...), molecular mass [37], polydispersity [39], traces of catalysts [40], crystallinity [38] and sample shape [41]. In this study, we report the hygrothermal ageing of two P(L)LA of different molecular weights and their blend with PεCL. One may notice that PεCL hygrothermal ageing is not studied, PεCL being melted in our set of experimental ageing conditions. P(L)LA/PεCL blend mechanical properties and water uptake are followed over ageing and characterized using different techniques such as thermal analysis, microscopic observations and size exclusion chromatography.

2. Experimental

2.1. Materials and blending conditions

2.1.1. Materials

Two P(L)LA were used, one from Unitika (Teramac TE-7000, Unitika Co.) $M_n = 123\,500$ Da, polydispersity index $I = 1.72$ (SEC, THF, $T = 25\text{ }^\circ\text{C}$), $T_g = 61\text{ }^\circ\text{C}$ and $T_m = 175\text{ }^\circ\text{C}$) noted P(L)LA^U and the other one from Nature Works (P(L)LA 7000D $M_n = 179\,200$ Da, polydispersity index $I = 1.75$ (SEC, THF, $T = 25\text{ }^\circ\text{C}$), $T_g = 58\text{ }^\circ\text{C}$ and $T_m = 152\text{ }^\circ\text{C}$) noted PLA^{NW}. PεCL was supplied by Solvay (CAPA 6500, Solvay, $M_n = 114\,200$ Da, polydispersity index $I = 1.3$ (SEC, THF, $T = 25\text{ }^\circ\text{C}$), $T_g = -60\text{ }^\circ\text{C}$, $T_m = 59\text{ }^\circ\text{C}$). The selected blends for this study were P(L)LA^U/PεCL w:w 80/20, P(L)LA^{NW}/PεCL w:w 80/20, noted respectively P(L)LA^U/PεCL and P(L)LA^{NW}/PεCL.

2.1.2. Processing conditions

Drying of pellets was performed for 8 h at $50\text{ }^\circ\text{C}$ under reduced pressure before use. A twin-screw extruder (Clextral 900 mm) with co-rotating screws was used for melt blending. Temperature was set at $170\text{ }^\circ\text{C}$, speed rate was kept at 250 rpm and feed rate was 4 kg/h. A dry blend of the polyesters was introduced to the extruder with the help of a feeder. The extrudate was pelletized and injection-molded to obtain tensile test samples. The injection-molding was performed using a Sandretto/95 t. Temperature was set at $170\text{ }^\circ\text{C}$, speed rate was kept at 30 rpm and cycles were 67 s long.

2.2. Mechanical properties: tensile and impact measurements

Mechanical properties were measured after conditioning the samples at room temperature under standard atmospheric conditions ($22\text{--}24\text{ }^\circ\text{C}$) for 72 h before testing. Elongation at break was measured according to the ISO 527 standard (crosshead speed: 50 mm/min) using a Zwick Z100 tensile testing machine (load cell range 0–10 kN). The values recorded were the average of at least five specimens. Unnotched Charpy impact strength was determined using a Zwick apparatus according the ISO 179 standard (2 J, 4 J and 7.5 J). Testing was done on specimens of $80 \times 10 \times 4\text{ mm}^3$.

2.3. Hygrothermal ageing

2.3.1. Ageing conditions

Generally, hygrothermal ageing refers to the process in which the deterioration of the mechanical performance and integrity of materials results from the combined action of moisture and temperature [24]. A temperature above glass transition and high relative humidity (RH) environment can accelerate many failure mechanisms of polymers. In this study, hygrothermal environment was $65\text{ }^\circ\text{C}/100\%$ RH. A hole made at the very top of each bar made it possible to fix them vertically above the surface of distilled water in a stainless steel autoclave. Tests have been carried out for ageing times of 0, 6, 24, 48, 120 and 240 h.

2.3.2. Water uptake

Water uptake was measured by weighing five samples right after the end of each ageing at ambient temperature. Weight gains were recorded by weighing on a balance with a precision of 1 mg. The percentage gain at any time t , M_t as a result of moisture absorption, was determined by Eq. (1):

$$M_t(\%) = \frac{(W_w - W_d)}{W_d} \quad (1)$$

where W_d and W_w denote, respectively, weight of dry material (the initial weight of materials prior to exposure to the water absorption) and weight of materials after exposure to water absorption.

2.4. Thermal analysis

DSC experiments were performed on Perkin Elmer (Pyris Diamond) equipment, calibrated with indium and zinc standards and data were recorded at a heating rate of $10\text{ }^\circ\text{C}/\text{min}$. Sample sizes were 6–8 mg, and they were analyzed in standard aluminium DSC pans. Prior to the measurement, the baseline was established with two empty pans. Oxidation was prevented by circulating nitrogen gas around the samples during analysis. The samples were heated from -90 to $190\text{ }^\circ\text{C}$. The first scan was studied in order to measure sample crystallinities and relate them to mechanical properties. Three samples taken from the middle of three different bars where tested. With the maximum of the endothermic peak detected on heating scans being taken as the melting temperature, the peak area was used to calculate the enthalpy of melting using Pyris 8.0 software. The crystallinities of P(L)LA $X_c(\text{P(L)LA})$ and PεCL $X_c(\text{PεCL})$ were calculated using the following Eq. (2):

$$X_c(\%) = \frac{(\Delta H_m - \Delta H_{cc})}{\omega \Delta H_m^0} \quad (2)$$

where ΔH_m , ΔH_m^0 and ΔH_{cc} (J/g of polymer) and ω , are respectively the melting enthalpy, the melting enthalpy of infinite thickness crystal, the cold crystallization enthalpy and the weight fraction of

each component. We used $\Delta H_m^0(\text{P(L)LA}) = 106 \text{ J/g}$ [42] and $\Delta H_m^0(\text{P(L)LA}^{\text{NW}}) = 139 \text{ J/g}$ [43].

2.5. Environmental scanning electron microscopy

The morphology of the polymer blends was examined with a QUANTA 200 FEG (FEI Company) environmental scanning electron microscope. Injection-molded bars were fractured in liquid nitrogen and stuck to aluminium stubs. In order to prevent P(L)LA degradation by the electron beam, samples were then coated with carbon using a Carbon Evaporation Device CED030 (Balzers). Once the pressure was obtained ($P = 10^{-2}$ mbar) the coating was carried out for 15 min. The thickness of the carbon layer obtained was around 15 nm. ESEM experimental observation conditions were very low pressure (around 10^{-7} Torr), voltage 2–5 kV and work distance 8 mm.

2.6. Size exclusion chromatography

Molecular weights were determined by size exclusion chromatography (SEC) using a Waters equipment fitted with a 60 cm long column equipped with PLgel as the stationary phase, THF at $1 \text{ cm}^3/\text{min}$ flow rate as the mobile phase, and a Waters 410 refractometric detector, as reference to polystyrene standards. Typically, polymer (10 mg) was dissolved in 2 cm^3 of THF and the resulting solution was filtered on a 0.45 mm Millipore filter before injection of 20 mL of sample solution. M_n and M_w are expressed according to calibration using polystyrene standards.

3. Results and discussion

3.1. Comparison of P(L)LA^U and P(L)LA^{NW} properties

3.1.1. Water absorption

Fig. 1 shows water uptake of P(L)LA^U and P(L)LA^{NW} as a function of hydrothermal ageing time. For both types of polymers the evolution of water uptake could be divided in two parts: a first part related to a Fickian behavior of water absorption, characterized by a non-linear increase, up to 24 h of ageing followed by a plateau, regardless of the crystallinity or molecular weight of the samples. Literature had previously reported P(L)LA water absorption Fickian behavior [44]. The second part of the curve, above 120 h of ageing corresponds to a significant water uptake increase from 0.8% to 1.4% for P(L)LA^{NW} and from 0.6% to 1.2% for P(L)LA^U. Water uptake increases at long ageing times are probably associated with osmotic cracking phenomenon [45]. An osmotic cracking phenomenon

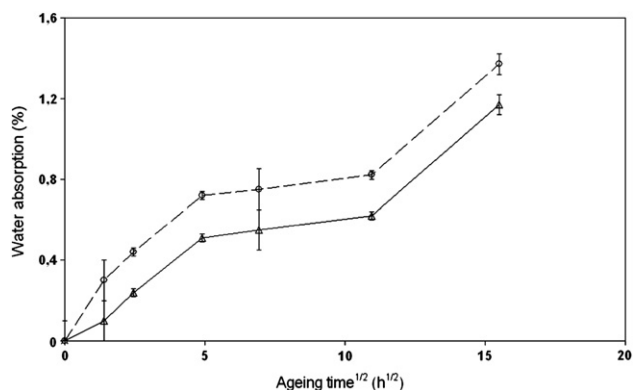


Fig. 1. Water absorption of P(L)LA^U and P(L)LA^{NW} as a function of hydrothermal ageing (○) neat P(L)LA^{NW}; (△) P(L)LA^U.

originates from an influx of water into the polymer matrix inducing an osmotic pressure, due to formed oligomer poor diffusivity and strong water affinity for these hydrophilic oligomer solutes within the polymer matrix. One would expect that P(L)LA^{NW} higher molecular weight compared to P(L)LA^U would be related to lower water uptakes since P(L)LA^{NW} chain mobility would be lower, thus inducing a lower diffusion of water molecules in the polymer. But, eventually our results highlighted that crystallinity seemed to be the most significant factor as $X_c(\text{P(L)LA}^{\text{U}})$ was higher than $X_c(\text{P(L)LA}^{\text{NW}})$ thus possibly reducing chain mobility and water diffusion for P(L)LA^U based blends.

3.1.2. Crystallinity

DSC first heating scans are given for P(L)LA^U and P(L)LA^{NW} as a function of ageing time in Table 1. Before ageing the glass transition temperatures (T_g) are respectively around 65°C and 61°C , for P(L)LA^U and P(L)LA^{NW}, cold crystallization temperature T_{cc} are respectively 104°C and 97°C while P(L)LA^U has a crystallization-melting temperature T_{cm} at 158°C . The intensity of the later phenomenon is very small compared to those of cold crystallization and melting peak. Finally melting temperatures are 174°C for P(L)LA^U and 151°C for P(L)LA^{NW}. Crystallinities of both P(L)LA (Fig. 2) increased as a function of ageing time before reaching a plateau at 120 h. Although the initial crystallinities and the trend over ageing were very similar for each P(L)LA, their crystallinities for comparable ageing times, and particularly when reaching the plateau, were significantly different. Indeed, for long ageing time, $X_c(\text{P(L)LA}^{\text{U}}) = 42\%$ while $X_c(\text{P(L)LA}^{\text{NW}}) = 28\%$. P(L)LA^U higher crystallization compared to P(L)LA^{NW} may originate from P(L)LA^U possible higher enantiomeric purity, meaning that L/D lactide enantiomer ratio would be higher in P(L)LA^U than in P(L)LA^{NW}. Since we did not have the opportunity to characterize our P(L)LA lactide enantiomeric ratio, we can not conclude on this point. Besides, literature showed that hydrolysis of P(L)LA results in an increase of crystallinity [37] thanks to chemicrystallization which corresponds to the crystallization of degraded chains of polymer. At this point, one may wonder whether P(L)LA^U higher crystallinity, during ageing, could originate from a higher chemicrystallization due to a possible higher hydrolysis of P(L)LA^U compared to P(L)LA^{NW}. This hypothesis was not corroborated by SEC measurements which showed that both polymers molecular weight decreased comparatively (see Fig. 5). Concerning P(L)LA melting temperatures, they

Table 1

DSC parameters obtained from the first heating scan for neat P(L)LA^U (a) and neat P(L)LA^{NW} (b) as a function of ageing.

(a)								
P(L)LA ^U / ageing time	T_g ($^\circ\text{C}$)	T_{cc1} ($^\circ\text{C}$)	ΔH_{cc1} (J/g)	T_{cm} ($^\circ\text{C}$)	ΔH_{cc2} (J/g)	T_m ($^\circ\text{C}$)	ΔH_m (J/g)	γ_c (%)
0	63.1	104	24.9	157.9	1.2	174.5	33.4	6.8
2	61.2	97	20.8	156.4	0.6	174.2	33.6	11.7
6	62.4	98.2	10	155.7	1.2	174.3	43.5	30.5
24	60.5	77	2.5	155.2	1.6	174.4	39.5	33.4
48	61.3	76	0.1	–	–	173.7	40.1	37.1
120	60.4	75	0.1	–	–	171.5	45.4	42.8
240	60.3	76	0.1	–	–	171.1	48.3	45.6
(b)								
P(L)LA ^{NW} / ageing time	T_g ($^\circ\text{C}$)	T_{cc1} ($^\circ\text{C}$)	ΔH_{cc1} (J/g)	T_m ($^\circ\text{C}$)	ΔH_m (J/g)	γ_c (%)		
0	61.3	97	12.8	151.7	17	3.9		
2	60.7	98.5	10.5	150.1	16	5.2		
6	61.1	98.9	8.4	149.9	16.4	7.5		
24	61.1	–	–	151.4	9.4	8.9		
48	59.7	–	–	149.8	26.3	24.8		
120	59.3	–	–	150.4	29.3	27.6		
240	61.3	–	–	149	29.3	27.6		

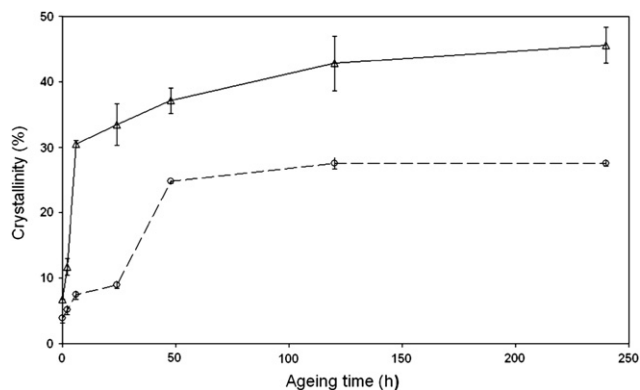


Fig. 2. Crystallinity of P(L)LA^U and P(L)LA^{NW} as a function of hydrothermal ageing (○) neat P(L)LA^{NW}; (△) P(L)LA^U.

remained constant, throughout hydrothermal ageing, showing that the crystalline phases obtained by annealing at 65 °C were very similar to the one obtained at cooling after molding, and that crystalline lamellae was not significantly attacked by hydrolysis. Finally, one may relate P(L)LA^U lower water uptake, highlighted previously, to its higher crystallinity compared to P(L)LA^{NW}.

3.1.3. Mechanical properties: elongation at break and impact strength

The tensile elongation at break of P(L)LA^U and P(L)LA^{NW} are given in Fig. 3. Both polymers had low initial elongation at break, making it difficult to compare the evolution of this property as a function of ageing time. Both polymer elongations at break decreased proportionally to ageing time. Fig. 4 follows the evolution of impact strength during ageing. P(L)LA^{NW} initial impact strength was higher than the one of P(L)LA^U. This difference was observed throughout ageing except for long ageing time (240 h) when impact strengths became almost identical. We can assume that P(L)LA^{NW} better impact strength was mainly related to its lower crystallinity and higher molecular weight. Both polymer impact strengths lowered down during ageing. Still, in the case of P(L)LA^{NW} this decrease was drastic above 120 h of ageing while for P(L)LA^U a linear decrease was observed. The evolution of impact strength during ageing can be related to water absorption. Indeed, whereas no plasticization effect was observed throughout ageing, chemical degradation was highlighted by SEC. One should note that both molecular weight and impact strength had comparable evolutions as a function of time.

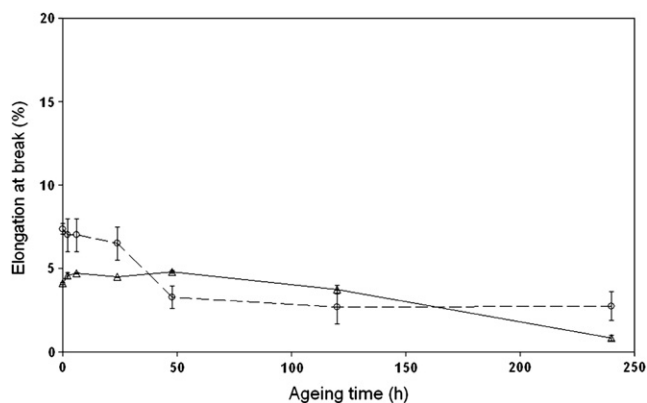


Fig. 3. Elongation at break of P(L)LA^U and P(L)LA^{NW} as a function of hydrothermal ageing (○) neat P(L)LA^{NW}; (△) P(L)LA^U.

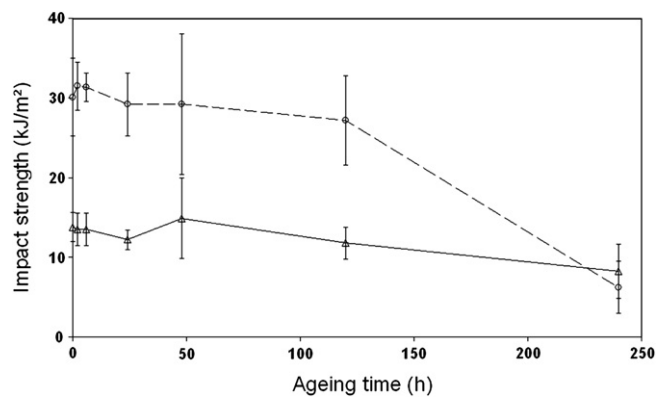


Fig. 4. Impact strength of P(L)LA^U and P(L)LA^{NW} as a function of hydrothermal ageing (○) neat P(L)LA^{NW}; (△) P(L)LA^U.

3.1.4. Molecular weight evolution

Size Exclusion Chromatography measurements showed that both polymer molecular weights decreased very comparatively (see Fig. 5), regardless of their initial molecular weights and their initial crystallinities. The evolution of molecular weight in the case of an autocatalytic hydrolysis reaction is given by Eq. (3):

$$\ln M_{n,t} = \ln M_{n,0} - kt \quad (3)$$

$M_{n,t}$ is the number average molecular weight at time t , $M_{n,0}$ is the number average molecular weight at time zero, and k is the hydrolysis rate constant. This kinetic was derived by Pitt et al. [46] and were again supported by Tsuji [47]. Results for P(L)LA^{NW} are $k = -1.25 \times 10^{-6} \text{ s}^{-1}$ (correlation coefficient $R^2 = 0.93$) and for P(L)LA^U are $k = -6.38 \times 10^{-7} \text{ s}^{-1}$ (correlation coefficient $R^2 = 0.92$). Those results are in good agreement with previous findings [48].

In addition, one may notice that P(L)LA^U higher water uptake compared to P(L)LA^{NW}, did not lead to higher degradation thus highlighting the complex connection between water uptake and hydrolysis.

3.2. Properties of P(L)LA/PεCL blends: P(L)LA^U/PεCL blends and P(L)LA^{NW}/PεCL blends

3.2.1. Water absorption

Figs. 6 and 7 show water uptake of P(L)LA^U/PεCL and P(L)LA^{NW}/PεCL as a function of hydrothermal ageing time. For both types of P(L)LA, water uptakes were different from the neat homopolymers. Even though a non-linear initial increase followed by a plateau, both related to water absorption Fickian behavior, were observed,

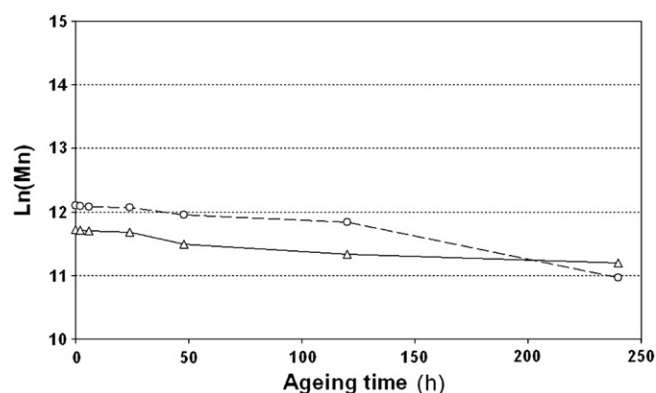


Fig. 5. Plot $\ln(M_n)$ versus ageing time for neat (△) P(L)LA^U and neat (○) P(L)LA^{NW}.

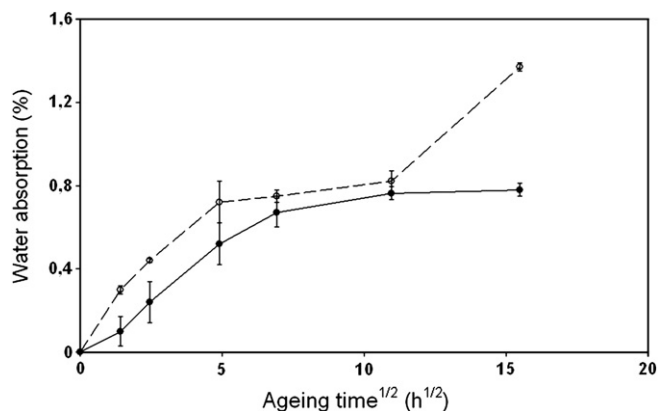


Fig. 6. Effect of blending with P ϵ CL on P(L)LA^{NW} based blend water absorption as a function of hydrothermal ageing (\circ) P(L)LA^{NW}; (\bullet) P(L)LA^{NW}/P ϵ CL.

no water uptake increase, at 240 h of ageing, was identified for both P(L)LA/P ϵ CL blends. This means that the osmotic cracking phenomenon observed on P(L)LA might not occur. This observation could be justified in that water molecules may have gone preferably into P ϵ CL [38], thus reducing the degradation and the formation of P(L)LA oligomers. This hypothesis is plausible since our hydrothermal test was run at 65 °C, above P ϵ CL melting temperature, $T_m^{P\epsilon CL} = 59$ °C. Then, at 65 °C, regardless of P ϵ CL hydrophobicity, water molecules diffusivity should be more pronounced in P ϵ CL than in P(L)LA. Still, if this was true, one would anticipate that P(L)LA would degrade slower when blended to P ϵ CL than when pure. Unfortunately, we could not corroborate this hypothesis to P(L)LA based blend molecular weight. Indeed one single elution peak was observed for all blends, when using size exclusion chromatography. In addition, we failed to selectively extract P ϵ CL or P(L)LA from the blends in order to characterize them. Nevertheless, our study reports that for hydrothermal tests run at 65 °C, water uptakes over ageing were very similar when comparing P(L)LA/P ϵ CL blends to neat P(L)LA. In addition, for long ageing times (240 h) blend water uptakes were lower than neat P(L)LA.

3.2.2. Crystallinity

Fig. 8 represents the crystallinities of both blends as a function of ageing time while DSC first heating scans are listed as a function of ageing time in **Table 2**. DSC curves of P(L)LA^U/P ϵ CL and P(L)LA^{NW}/P ϵ CL showed that P ϵ CL and P(L)LA melting peaks were different, which was a proof of low compatibility of those two polymers. Besides $T_m^{P\epsilon CL} = 59$ °C, then hiding both P(L)LA glass transitions.

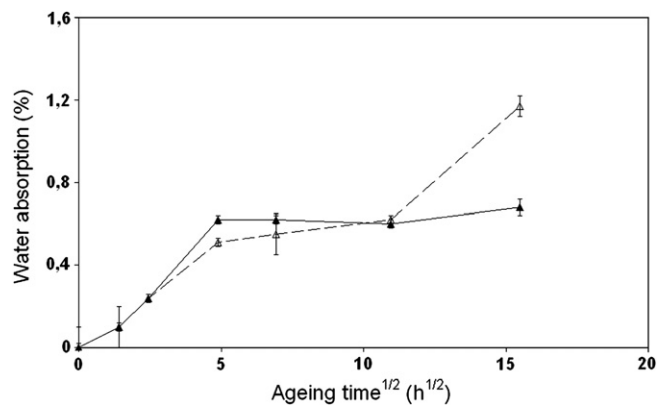


Fig. 7. Effect of blending with P ϵ CL on P(L)LA^U based blend water absorption as a function of hydrothermal ageing (Δ) P(L)LA^U; (\blacktriangle) P(L)LA^U/P ϵ CL.

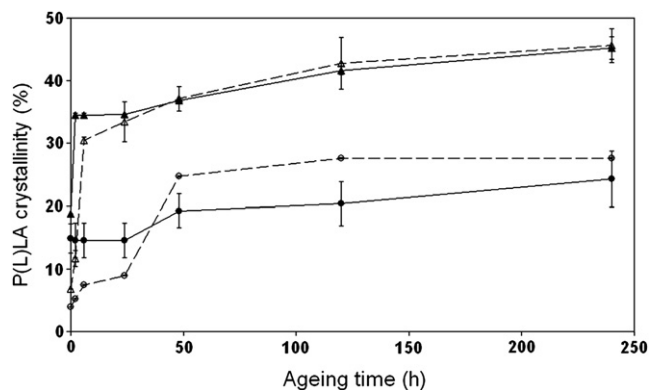


Fig. 8. Effect of blending with P ϵ CL on P(L)LA^{NW} and P(L)LA^U crystallinity as a function of hydrothermal ageing (Δ) P(L)LA^U; (\blacktriangle) P(L)LA^U/P ϵ CL; (\circ) P(L)LA^{NW}; (\bullet) P(L)LA^{NW}/P ϵ CL.

Before ageing, the initial crystallinities of the two blended P(L)LA were much higher than pure P(L)LA (about 40% for blends compared to about 5% for neat P(L)LA). Similar profiles of P(L)LA crystallinity have been observed in the literature [28] and were accredited to a typical nucleating effect of P ϵ CL on P(L)LA characterized by higher crystallization rates of blended P(L)LA. Yet, after

Table 2

DSC parameters obtained from the first heating scan for P(L)LA^U/P ϵ CL blend (a and b respectively) and P(L)LA^{NW}/P ϵ CL blend (c and d respectively) as a function of ageing time.

(a)								
P(L)LA ^{NW} /ageing time	T _g (°C)	T _{cc1} (°C)	ΔH_{cc1} (J/g)	T _m (°C)	ΔH_m (J/g)	χ_c (%)		
0	—	94.8	4.7	153.7	20.5	14.9		
2	—	95.9	4	153	19.3	14.4		
6	—	95.9	3.9	153	19.3	14.5		
24	—	95.9	0.5	153	15.9	14.5		
48	—	—	—	153	20.5	19.3		
120	—	—	—	152.7	21.6	20.4		
240	—	—	—	155.1	25.8	24.3		
(b)								
P ϵ CL/ageing time	T _m (°C)	ΔH_m (J/g)	χ_c (%)					
0	62.1	17.3	43.2					
2	61.3	16.3	45.7					
6	61.3	16.3	44.9					
24	61.3	16.3	44.9					
48	60.0	16.3	35.9					
120	58.5	17.3	31.5					
240	59.0	20.6	24.9					
(c)								
P(L)LA ^U /ageing time	T _g (°C)	T _{cc1} (°C)	ΔH_{cc1} (J/g)	T _{cm} (°C)	ΔH_{cc2} (J/g)	T _m (°C)	ΔH_m (J/g)	χ_c (%)
0	—	85.2	12.9	153.2	1.1	171.5	33.9	18.8
2	—	85.2	10.3	153.1	1	170.3	45.8	34.5
6	—	85.2	9.9	153	0.9	171.3	47.4	34.5
24	—	72.7	—	153.5	0.5	170.6	37.3	34.7
48	—	—	—	—	—	171.4	39	36.8
120	—	—	—	—	—	171.1	44.2	41.7
240	—	—	—	—	—	170.3	47.9	45.2
(d)								
P ϵ CL/ageing time	T _m (°C)	ΔH_m (J/g)	χ_c (%)					
0	61.6	9.3	33.3					
2	61.2	9.4	33.9					
6	61.2	9.4	33.9					
24	61.2	9.9	35.9					
48	61.2	11.0	39.6					
120	61.2	11.9	42.9					
240	61.2	12.3	44.4					

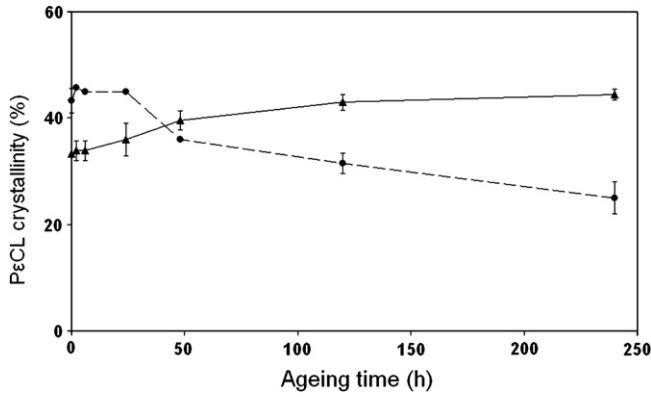


Fig. 9. P ϵ CL crystallinity when blended to P(L)LA^{NW} and P(L)LA^U as a function of hydrothermal ageing (▲) P ϵ CL in P(L)LA^U based blend; (●) P ϵ CL in P(L)LA^{NW} based blend.

hydrothermal ageing began, the crystallinities of blended P(L)LA became very similar to pure aged P(L)LA crystallinities. X_c increased as a function of ageing time before it reached a plateau at 120 h. Again, the trend over ageing was the same for each P(L)LA while the crystallinities at the plateau were significantly different depending on the type of P(L)LA, X_c (P(L)LA^U) being higher than X_c (P(L)LA^{NW}).

It was unexpected that, during ageing at 65 °C, P ϵ CL would not have increased P(L)LA crystallinity. In previous studies [28] the effect of P ϵ CL on P(L)LA occurs above 120 °C, which is typical of P(L)LA crystallization temperature [49] at cooling. At the temperature of 120 °C, blended P(L)LA crystallizes faster compared to pure P(L)LA, either because of a possible plasticization effect due to P ϵ CL oligomeric fractions or because of an heterogeneous nucleation effect of P ϵ CL on P(L)LA. In fact, in the later case, the interface of the phase-separated domains may provide favorable nucleation sites for crystallization and therefore, the crystallization rate of P(L)LA could be promoted by a nucleation barrier lower than that of pure P(L)LA melt [28]. But neither of those two phenomena were observed in our set of experimental ageing conditions at 65 °C, suggesting temperature may also impact on the ability of P ϵ CL to promote P(L)LA crystallization.

Concerning P ϵ CL initial crystallinity (Fig. 9), a slight dependence on P(L)LA molecular weight was observed since X_c (P ϵ CL) = 35% in P(L)LA^U/P ϵ CL and X_c (P ϵ CL) = 42% in P(L)LA^{NW}/P ϵ CL. Besides, the evolution of P ϵ CL crystallinity as a function of ageing time could not be interpreted easily as P ϵ CL was melted during ageing at 65 °C. Besides, throughout hydrothermal ageing both blended P(L)LA

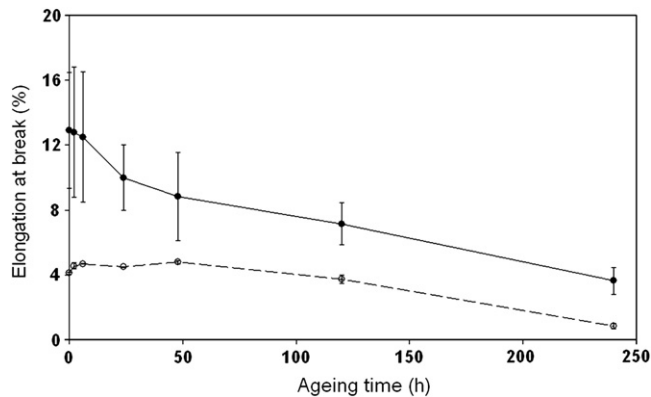


Fig. 10. Effect of P ϵ CL on P(L)LA^{NW} based blend elongation at break as a function of hydrothermal ageing (○) neat P(L)LA^{NW}; (●) P(L)LA^{NW}/PCL.

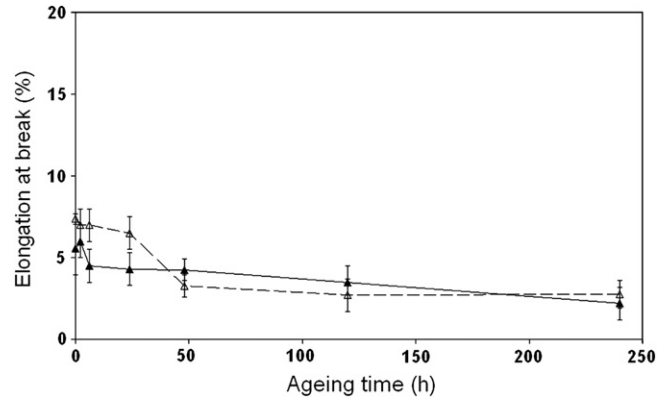


Fig. 11. Effect of P ϵ CL on P(L)LA^U based blend elongation at break as a function of hydrothermal ageing (△) neat P(L)LA^U; (▲) P(L)LA^U/PCL.

melting temperatures remained constant and respectively equal to virgin P(L)LA, showing that annealing did induce the same crystalline phases.

3.2.3. Mechanical properties: elongation at break and impact strength

The tensile elongation at break of P(L)LA^U/P ϵ CL and P(L)LA^{NW}/P ϵ CL are given in Figs. 10 and 11. Both blends had low initial elongations at break, making it difficult to conclude on the effect of morphology on this particular property. Anyway, while initial elongation of P(L)LA^{NW}/P ϵ CL was higher than pure P(L)LA^{NW}, the elongation of P(L)LA^U/P ϵ CL was pretty much the same than pure P(L)LA^U. Literature observed that for tensile bars made out of P(L)LA/P ϵ CL immiscible blends, the degree of mixing and the crystallinity were critical parameters of the elongation at break [37]. Our results showed that P(L)LA^{NW} crystallinity was enhanced when blended to P ϵ CL which did not account for its relatively improved elongation at break. Still, P(L)LA^U crystallinity remained the same when blended to P ϵ CL, explaining somehow that its elongation at break was not improved. For both blends, elongation at break decreased proportionally to ageing time, showing no special evidence of any plasticization effect due to water in the polymers. Figs. 12 and 13 give the evolution of impact strength for P(L)LA^U/P ϵ CL and P(L)LA^{NW}/P ϵ CL during ageing. It is clear that P(L)LA^U/P ϵ CL impact strength did not differ significantly from pure P(L)LA^U. However, P(L)LA^{NW}/P ϵ CL initial impact strength was higher than pure P(L)LA^{NW}. At this point, it is interesting to notice that for P(L)LA^{NW} based blends, P(L)LA^{NW} initial crystallinity was higher

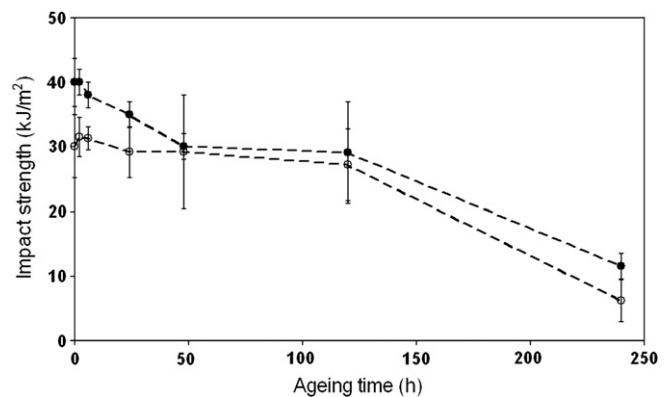


Fig. 12. Effect of P ϵ CL on P(L)LA^{NW} based blend impact strength as a function of hydrothermal ageing (○) neat P(L)LA^{NW}; (●) P(L)LA^{NW}/PCL.

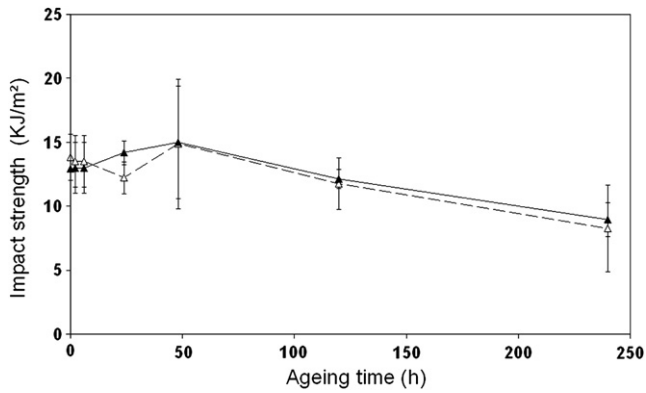


Fig. 13. Effect of PεCL on P(L)LA^U based blend impact strength as a function of hydrothermal ageing (Δ) P(L)LA^U; (\blacktriangle) P(L)LA^U/PεCL.

compared to pure P(L)LA^{NW}. While one would expect impact strength to drop down proportionally to crystallinity it was the opposite that was observed with P(L)LA^{NW}. This phenomenon is probably associated with the level of mixture of two components developed during extrusion. Finally, for P(L)LA^{NW}/PεCL one could also assume that this aptitude of elongation could be related to the presence of PεCL in the matrix and to its good level of mixture or to a better interaction between P(L)LA^{NW} and PεCL than between P(L)LA^U and PεCL. The evolution of P(L)LA^{NW}/PεCL impact strength was as follows, first a non-linear decrease followed by plateau after 48h of ageing, regardless of the crystallinity or molecular weight of the samples. Then above 120 h, impact strength decreased drastically. One may notice that before 120 h, the evolution of impact strength

followed almost the same trend than water absorption, which could be related to hydrolysis or decohesion of the blend. While, above 120 h, impact strength decreased strongly, no variation of water uptake was observed, then highlighting the competition of different phenomena in the evolution of impact strength.

3.2.4. Morphology

Environmental scanning electron microscopy was used to investigate the microstructure, as a function of ageing (Fig. 14), of P(L)LA^U/PεCL and P(L)LA^{NW}/PεCL blends. The initial microstructure of both blends was characterized by relatively small spherical inclusions of what was assumed to be PεCL in P(L)LA matrix (see (a) and (c)). The particles had diameters ranging from 0.3 μm to 0.6 μm and appeared to be isolated from each other by the matrix. Initial interfaces between the spherical inclusions and the matrix appeared to be sharp, suggesting there was little adhesion between the two phases for both blends. Those observations are consistent with the fact that P(L)LA and PεCL have fairly close thermal expansion coefficients and a difference in solubility parameter of less than one [50]. Anyway, thermodynamic compatibility between P(L)LA and PεCL is expected to be very small. Even though solubility parameters of the two hydrophobic polyesters are close suggesting the possibility of some degree of phase mixing, no significant acid–base interaction and/or hydrogen bonding between the two components can be expected thus accounting for the phase-separated domain structure [28].

The evolution of morphology over ageing showed decohesion of the spherical inclusions from the main matrix for both blends. This phenomenon was particularly obvious for long ageing time such as 240 h (see (b) and (d)).

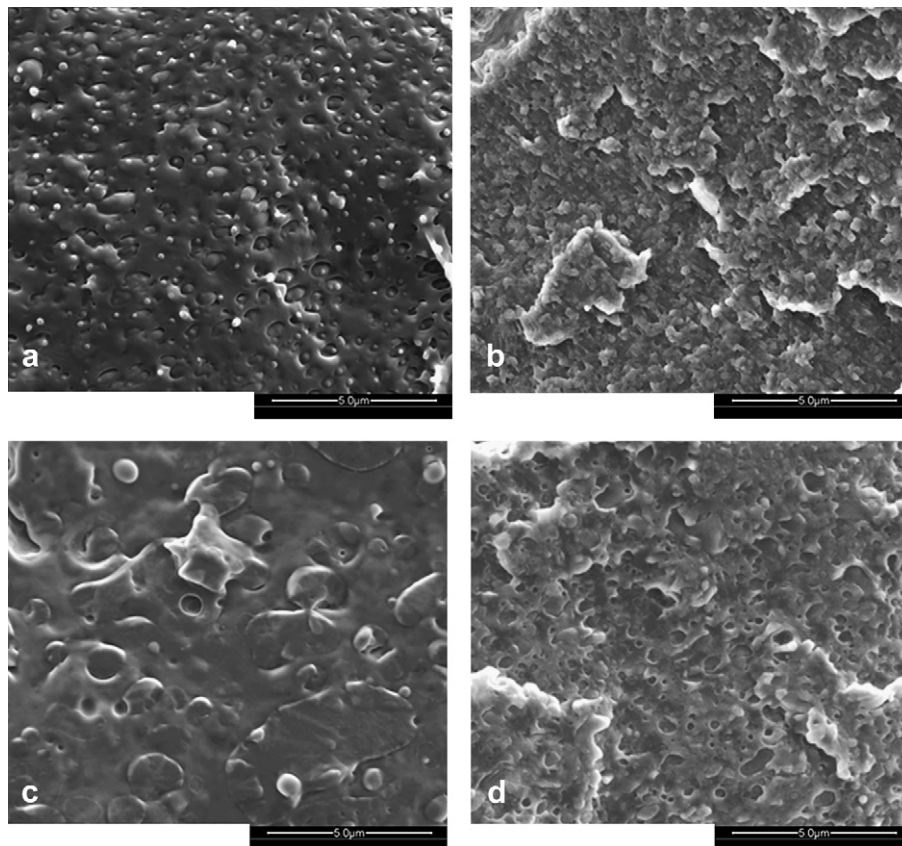


Fig. 14. ESEM fractured under liquid nitrogen as a function of ageing time P(L)LA^U/PεCL, before ageing (a), P(L)LA^U/PεCL, after 240 h of ageing (b), P(L)LA^{NW}/PεCL, before ageing (c) and P(L)LA^{NW}/PεCL, after 240 h of ageing (d).

4. Conclusions

In the present study P(L)LA/PεCL w:w 80/20 blends were subjected to accelerated ageing using two P(L)LA of different molecular weight, to estimate their long-term hygrothermal stability compared to pure P(L)LA. Blending of polymer was found to constitute a simple means by which initial elongation and resilience could be improved compared to pure P(L)LA regardless of P(L)LA initial crystallinity enhancement upon blending. During ageing, increases in crystallinity seemed to lower water uptake at short ageing times, while osmotic cracking was found to occur in pure P(L)LA for long ageing times but not in P(L)LA/PεCL blends. Blended P(L)LA crystallinities throughout ageing were very similar to pure P(L)LA. While P(L)LA resilience decrease could be related to chain scission, blend aptitude to elongations decrease could only be related to interphase decohesion at long ageing times. Eventually blend elongation at break and resilience became very comparable to pure aged P(L)LA. Finally, It would be of interest to optimize the blending conditions possibly using reactive blending, in order to investigate blend morphology and water resistance in details as long as those blends would remain biodegradable even if chemically modified.

References

- [1] Smith R, editor. Biodegradable polymers for industrial applications. London: CRC Press; 2005.
- [2] Stolt M, Viljanmaa M, Södergård A, Törmälä P. Blends of poly(ε-caprolactone-*b*-lactic acid) and poly(lactic acid) for hot-melt applications. *J Appl Polym Sci* 2004;91(1):196–204.
- [3] Vanionpää A, Rokkanen P, Törmälä P. *Prog Polym Sci* 1989;14(5):679–716.
- [4] Nakagawa M, Teraoka F, Fujimoto S, Hamada Y, Kibayashi H, Takahashi J. Improvement of cell adhesion on poly(L-lactide) by atmospheric plasma treatment. *J Biomed Mater Res* 2006;77A(1):112–8.
- [5] Amass W, Amass A, Tighe B. A review of biodegradable polymers: uses, current developments in the synthesis and characterization of biodegradable polyesters, blends of biodegradable polymers and recent advances in biodegradation studies. *Polym Int* 1998;47(2):89–144.
- [6] Chen CC, Chueh JY, Tseng H, Huang HM, Lee SY. Preparation and characterization of biodegradable PLA polymeric blends. *Biomaterials* 2003;24(7):1167–73.
- [7] Avérous L. In: Belgacem N, Gandini A, editors. Monomers, polymers and composites from renewable resources. Poly(lactic acid): synthesis, properties and applications. Elsevier; 2008. p. 433–50 [chapter 21].
- [8] Carlotta D. A literature review of poly(lactic acid). *J Polym Environ* 2001;9(2):63–84.
- [9] Sheth M, Ananda Kumar R, Dave V, Gross RA, McCarthy SP. Biodegradable polymer blends of poly(lactic acid) and poly(ethylene glycol). *J Appl Polym Sci* 1997;66(8):1495–505.
- [10] Anderson KS, Lim SH, Hillmyer MA. Toughening of polylactide by melt blending with linear low-density polyethylene. *J Appl Polym Sci* 2003;89(14):3757–68.
- [11] Ljungberg N, Andersson T, Wesslen B. Film extrusion and film weldability of poly(lactic acid) plasticized with triacetone and tributyl citrate. *J Appl Polym Sci* 2003;88(14):3239–47.
- [12] Anderson KS, Hillmyer MA. The influence of block copolymer microstructure on the toughness of compatibilized polylactide/polyethylene blends. *Polymer* 2004;45(26):8809–23.
- [13] Anderson KS, Schreck KM, Lim SH, Hillmyer MA. Toughening polylactide. *Polym Rev* 2008;48(1):85–108.
- [14] Markarian J. Biopolymers present new market opportunities for additives in packaging. *Plast Add Comp* 2008;10(3):22–5.
- [15] Ikada Y, Jamshidi K, Tsuji H, Myon SH. Stereocomplex formation between enantiomeric poly-L-(lactides). *Macromolecules* 1987;20(4):904–6.
- [16] Meredith JC, Amis EJ. LCST phase separation in biodegradable polymer blends: poly(D, L-lactide) and poly(ε-caprolactone). *Macromol Chem Phys* 2000;201(6):733–9.
- [17] Jiang L, Wolcott MP, Zhang. Study of biodegradable polylactide/poly(butylene adipate-co-terephthalate) blends. *J Biomater Sci* 2006;7(1):199–207.
- [18] Ohkoshi I, Abe H, Doi Y. Miscibility and solid-state structures for blends of poly[(S)-lactide] with atactic poly[(R, S)-3-hydroxybutyrate]. *Polymer* 2000;41(15):5985–92.
- [19] Noda I, Satkowski MM, Dowrey AE, Marcott C. Polymer alloys of nodax copolymers and poly(lactic acid). *Macromol Biosci* 2004;4(3):269–75.
- [20] Shibata M, Inoue Y, Miyoshi M. Mechanical properties, morphology, and crystallization behavior of blends of poly(L-lactide) with poly(butylene succinate-co-L-lactate) and poly(butylene succinate). *Polymer* 2006;47(10):3557–64.
- [21] Lu J, Qiu Z, Yang W. Fully biodegradable blends of poly(L-lactide) and poly(ethylene succinate): miscibility, crystallization, and mechanical properties. *Polymer* 2007;48(14):4196–204.
- [22] Tsuji H, Yamada T, Suzuki M, Itsuno S. Blends of aliphatic polyesters. Part 7. Effects of poly(L-lactide-co-ε-caprolactone) on morphology, structure, crystallization, and physical properties of blends of poly(L-lactide) and poly(ε-caprolactone). *Polym Int* 2003;52(2):269–75.
- [23] Semba T, Kitagawa K, Ishiaku US, Kotaki M, Hamada H. Effect of compounding procedure on mechanical properties and dispersed phase morphology of poly(lactic acid)/polycaprolactone blends containing peroxide. *J Appl Polym Sci* 2007;103(2):1066–74.
- [24] Tsuji H, Ikada Y. Blends of aliphatic polyesters. II. Hydrolysis of solution-cast blends from poly(L-lactide) and poly(ε-caprolactone) in phosphate-buffered solution. *J Appl Polym Sci* 1998;67(3):405–15.
- [25] Yang JM, Chen HL, You JW, Hwang JC. Miscibility and crystallization of poly(L-lactide)/poly(ethylene glycol) and poly(L-lactide)/poly(ε-caprolactone) blends. *Polym J* 1997;29(8):657–62.
- [26] Hiljanen-Vainio M, Varpomaa P, Seppälä J, Törmälä P. Modification of poly(L-lactides) by blending: mechanical and hydrolytic behaviour. *Macromol Chem Phys* 1996;197(4):1503–23.
- [27] Choi NS, Kim CH, Cho KY, Park JK. Morphology and hydrolysis of PCL/PLLA blends compatibilized with P(LLA-co-CL) or P(LLA-*b*-CL). *J Appl Polym Sci* 2002;86(8):1892–8.
- [28] Dell'Erba R, Groeninckx G, Maglio G, Malinconico M, Migliozi A. Immiscible polymer blends of semicrystalline biocompatible components: thermal properties and phase morphology analysis of PLLA/PCL blends. *Polymer* 2001;42(18):7831–40.
- [29] Broz ME, VanderHart DL, Washburn NR. Structure and mechanical properties of poly(D, L-lactic acid)/poly(ε-caprolactone) blends. *Biomaterials* 2003;24(23):4181–90.
- [30] Sarazin P, Roy X, Favis BD. Controlled preparation and properties of porous poly(L-lactide) obtained from a co-continuous blend of two biodegradable polymers. *Biomaterials* 2004;25(28):5965–78.
- [31] Tsuji H, Ikada Y. Blends of aliphatic polyesters. I. Physical properties and morphologies of solution-cast blends from poly(DL-lactide) and poly(ε-caprolactone). *J Appl Polym Sci* 1996;60(13):2367–75.
- [32] Lopez-Rodriguez N, Lopez-Ariza A, Meaurio E, Sarasua JR. Crystallization, morphology, and mechanical behavior of polylactide/poly(ε-caprolactone) blends. *Polym Eng Sci* 2006;46(9):1299–308.
- [33] Maglio G, Migliozi A, Palumbo R, Immirzi B, Volpe MG. Compatibilized poly(ε-caprolactone)/poly(L-lactide) blends for biomedical uses. *Macromol Rapid Commun* 1999;20(4):236–8.
- [34] Witzke DR. Introduction to properties, engineering, and prospects of polylactide polymer. Ph.D. thesis, Chemical Engineering, Michigan State University; 1997.
- [35] Li S, McCarthy SP. Further investigations on the hydrolytic degradation of poly(DL-lactide). *Biomaterials* 1999;20(1):35–44.
- [36] Drumright E, Gruber PR, Henton DE. Poly(lactic acid) technology. *Adv Mater* 2000;12(23):1841–6.
- [37] Bastioli C, editor. Handbook of biodegradable polymers. Rapra Technology; 2005.
- [38] Li S, McCarthy SP. Influence of crystallinity and stereochemistry on the enzymatic degradation of poly(lactide)s. *Macromolecules* 1999;32(13):4454–6.
- [39] Tsuji H, Suzuyoshi K. Thermal degradation of polyacrylic acid in dilute aqueous solution. *Polym Degrad Stab* 2002;75(2):347–55.
- [40] Sodergard A, Stolt M. Properties of lactic acid based polymers and their correlation with composition. *Prog Polym Sci* 2002;27(6):1123–63.
- [41] Grizzi I, Garreau H, Li S, Vert M. Hydrolytic degradation of devices based on poly(L-lactic acid) size-dependence. *Biomaterials* 1995;16(4):305–11.
- [42] Sarasua JR, Lopez Arraiza A, Balerdi P, Maiza I. Crystallinity and mechanical properties of optically pure polylactides and their blends. *Polym Eng Sci* 2005;45(5):745–53.
- [43] Crescenzi V, Manzini G, Calzolari G, Borri C. Thermodynamics of fusion of poly-β-propiolactone and poly-ε-caprolactone. comparative analysis of the melting of aliphatic polylactone and polyester chains. *Eur Polym J* 1972;8(3):449–63.
- [44] Yew GH, Mohd Yusof AM, Mohd Ishak ZA, Ishiaku US. Water absorption and enzymatic degradation of poly(lactic acid)/rice starch composites. *Polym Degrad Stab* 2005;90(3):488–500.
- [45] Gautier L, Mortaigne B, Bellenger V, Verdu J. Osmotic cracking nucleation in hydrothermal-aged polyester matrix. *Polymer* 2002;41(7):2481–90.
- [46] Pitt CG, Jeffcoat AR, Zweidinger RA. Sustained drug delivery system. I. The permeability of poly(caprolactone), poly(DL-lactic acid), and their copolymers. *J Biomed Mater Res* 1979;13:497.
- [47] Tsuji H. Polylactides. In: Steinbüchel A, editor. Biopolymers, vol. 4. Wiley VCH; 2004 [chapter 5].
- [48] Mohd-Adnan AF, Nishida H, Shirai Y. Evaluation of kinetics parameters for poly(L-lactic acid) hydrolysis under high-pressure steam. *Polym Degrad Stab* 2008;93(5):1053–8.
- [49] Li H, Huneault MA. Effect of nucleation and plasticization on the crystallization of poly(lactic acid). *Polymer* 2007;48(23):6855–66.
- [50] Park TG, Cohen S, Langer R. Poly(L-lactide acid)/pluronic blends: characterization of phase separation behavior, degradation, and morphology and use as protein-releasing matrixes. *Macromolecules* 1992;25(1):116–22.